

Journal of Materials Chemistry A

Accepted Manuscript



This is an *Accepted Manuscript*, which has been through the Royal Society of Chemistry peer review process and has been accepted for publication.

Accepted Manuscripts are published online shortly after acceptance, before technical editing, formatting and proof reading. Using this free service, authors can make their results available to the community, in citable form, before we publish the edited article. We will replace this *Accepted Manuscript* with the edited and formatted *Advance Article* as soon as it is available.

You can find more information about *Accepted Manuscripts* in the [Information for Authors](#).

Please note that technical editing may introduce minor changes to the text and/or graphics, which may alter content. The journal's standard [Terms & Conditions](#) and the [Ethical guidelines](#) still apply. In no event shall the Royal Society of Chemistry be held responsible for any errors or omissions in this *Accepted Manuscript* or any consequences arising from the use of any information it contains.

ARTICLE

A water-based and high space-time yield synthetic route to MOF Ni₂(dhtp) and its linker 2,5-dihydroxyterephthalic acid.

Cite this: DOI: 10.1039/x0xx00000x

Received 00th January 2012,
Accepted 00th January 2012

DOI: 10.1039/x0xx00000x

www.rsc.org/

Stéphane CADOT,^{a, b} Laurent VEYRE,^a Dominique LUNEAU,^c David FARRUSSENG,^d Elsjé Alessandra QUADRELLI^{a,*}

2,5-dihydroxyterephthalic acid (H₄dhtp) was synthesized in a 18g-scale by carboxylation of hydroquinone in molten potassium formate. The hydrated form of Ni₂(dhtp) MOF (also known as CPO-27-Ni and MOF-74(Ni)), was obtained in 92% yield by refluxing for 1h a water suspension of the H₄dhtp linker with an aqueous solution of nickel acetate. The ensuing characterization of the material (XRD, HRTEM, TGA, N₂ adsorption at 77K - S_{BET} = 1233 m²/g) confirmed the obtention of a metal-organic framework of at least equal quality than the ones obtained from the previously reported routes (CPO-27-Ni and MOF-74(Ni)), with a different morphology (namely, well-separated 1 μm platelets for the herein reported water-based route). The temperature dependence of the magnetic susceptibility was measured and satisfactorily simulated assuming a Heisenberg ($H = -2J\sum S_i S_{i+j}$) ferromagnetic intrachain interaction ($J = +8.1 \text{ cm}^{-1}$) with antiferromagnetic interchain interaction ($J' = -1.15 \text{ cm}^{-1}$). Overall, the reaction in water appears to follow easily distinguishable steps, the first being the deprotonation of H₄dhtp by acetate counterion, leading to a soluble nickel adduct of the linker, *en route* to the MOF self-assembly.

Introduction

Metal-Organic Frameworks (MOFs) have received considerable attention over the past decade, especially in the field of gas purification and storage as well as catalysis and drug delivery¹. The growing interest for these materials recently led to the first industrial production of MOFs with the ton-scale

synthesis of aluminum fumarate (Basolite A520[®]) at BASF facilities² which is a promising candidate for methane storage and delivery. This transfer to industrial production has been achieved, *inter alia*, through the development of a water-based route, reducing both production costs and environmental impact while increasing the production rates. Unfortunately, entirely water-based MOF synthesis are still very limited²⁻⁶.

Among the wide diversity of MOFs, the M₂(dhtp) series (dhtp = dobdc = 2,5-dioxido-1,4-benzenedicarboxylate [O₂C-C₆H₂O₂-CO₂]⁴⁻; M = Mg, Mn, Fe, Co, Ni or Zn)⁷, called CPO-27-M (CPO = Coordination Polymer of Oslo) or MOF-74(M), has been extensively studied because of its 1D microporous hexagonal channel structure with calibrated pores at 12 Å which allow an optimal interaction between the walls of the solid and guest molecules. In fact, M₂(dhtp) offers a permanent porosity upon solvent removal, displaying strong adsorption centers at the penta-coordinated open metal sites (see **Scheme 1** for M = Ni) which allow the selective adsorption/desorption of a wide diversity of molecules without loss of porosity⁸⁻¹⁰. In particular the nickel member of the M₂(dhtp) series, which is highly tolerant towards moisture¹¹ and oxygen¹², is able to

^a Laboratoire de Chimie Organométallique de Surface, C2P2 - UMR 5265 (CNRS - Université Lyon 1 - CPE Lyon), CPE Lyon, 43 Boulevard du 11 Novembre 1918, 69616 Villeurbanne Cedex

^b CEA, LETI, MINATEC Campus, F-38054 Grenoble, France

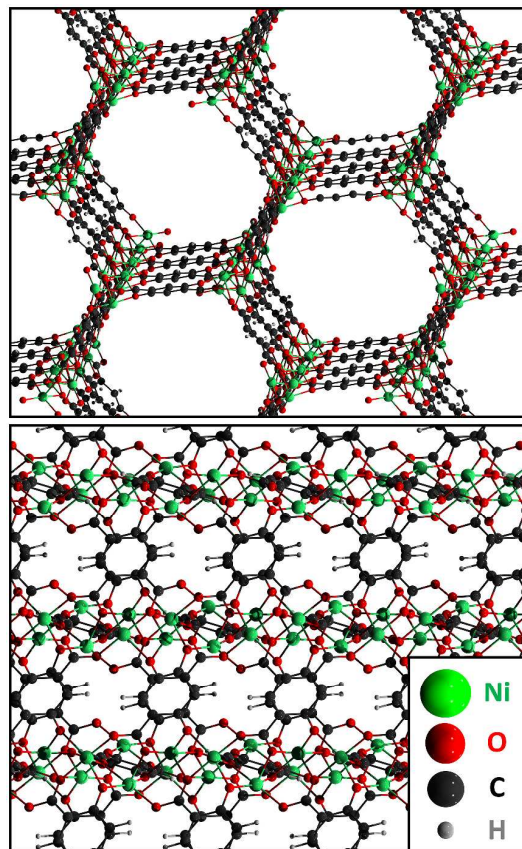
^c Laboratoire des Multimatériaux et Interfaces - UMR 5615 (Université Claude Bernard Lyon 1), Campus de La Doua, 69622 Villeurbanne Cedex

^d Institut de Recherche sur la Catalyse et l'Environnement de Lyon (IRCELYON), 2 Av. Albert Einstein, 69626 Villeurbanne cedex

*corresponding author: quadrelli@cpe.fr

† Electronic Supplementary Information (ESI) available: Experimental and simulated nitrogen adsorption and desorption isotherms at 77K and thermogravimetric analysis (TGA) under N₂ and O₂ of Ni₂(dhtp) as well as XRD diffraction pattern of the intermediate isolated along the synthesis described in the main text. See DOI: 10.1039/b000000x/

reversibly adsorb sulfur-containing molecules like H_2S^{13} or thiophene¹⁴, perform the selective adsorption of CO and CO_2 over CH_4 and $\text{H}_2^{9, 10}$ and of CO_2 over N_2 even under 3% relative humidity¹⁵ while the efficiency of this separation using $\text{Mg}_2(\text{dhtp})$ or zeolites is much more affected by only trace amount of water^{16, 17}. Most strikingly, $\text{Ni}_2(\text{dhtp})$ methane storage capacity is among the highest reported for MOFs ($214 \text{ cm}^3(\text{STP})/\text{cm}^3$ at 25°C , 35 bars)¹⁸, which makes it a very promising candidate for adsorption and/or separation applications. $\text{Ni}_2(\text{dhtp})$ is also active as Lewis-type catalyst¹⁹ and its application for delivering an anticancer drug²⁰ as well as its use in antimicrobial NO-delivering patch²¹ has been reported.



Scheme 1: Representation of the fully desolvated $\text{Ni}_2(\text{dhtp})$ structure²² showing the hexagonal 1D channels (upper picture : view towards (113) plane, lower picture : view towards (-120) plane).

Overall, MOF syntheses, there included $\text{Ni}_2(\text{dhtp})$ synthetic routes reported so far^{12, 22, 23} (see results section below for details), require high dilution factors which imply large amounts of organic solvents, low production rates and strong environmental impact. This is mainly ascribed to the difficulty to find a good solvent for both the metal salt and the organic linker. Therefore, not optimized small-scale lab syntheses as described in the literature have usually space-time yields (STY) between 0.1 and $1 \text{ kg}/\text{m}^3/\text{day}$ or even lower¹⁰. While reaction time has been reduced by one order of magnitude using

ultrasounds or microwave heating²⁴, the minimization of solvent usage is still a goal to attain with a STY larger than $500 \text{ kg}/\text{m}^3/\text{day}$. Beyond this, the development of water-based routes for MOF synthesis would strongly facilitate their industrialization. Indeed, organic solvents are more difficult to use at industrial levels because they shall be handled in specific non-flammable area, while water is a cheap, safe and more easily post-treatable solvent.

Here we report for the first time the synthesis of $\text{Ni}_2(\text{dhtp})$ in water with high space-time yield. We carefully demonstrate the quality of the obtained $\text{Ni}_2(\text{dhtp})$ by a series of characterization at short and long range, as well as its porous structure and not yet reported magnetic properties. In addition, we describe a synthesis method in a single step of the H_4dhtp linker from hydroquinone (which is a bulk chemical) using a cheap and organic solvent-free procedure. Indeed, 2,5-dihydroxyterephthalic acid is distributed in gram scale by different chemical suppliers at a price of about \$15 per gram. Although it does not represent the price at industrial level, it strongly limits its synthesis at kg scale for demonstration purposes.

Results and discussion

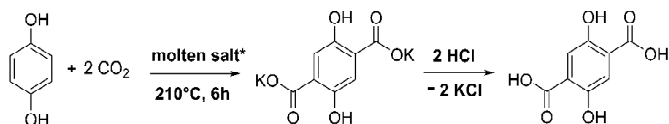
Two different synthetic routes have been reported for the isomorphous family of $\text{M}_2(\text{dhtp})$, both of them requiring organic solvents : tetrahydrofuran (THF) for the CPO-27 material originated from SINTEF's work in Oslo²² and dimethylformamide (DMF) (or DMF/water or DMF/water/ethanol mixtures) for the MOF-74²³ developed by Yaghi's group. The general procedure consists in mixing an aqueous solution of the metal salt with a solution of 2,5-dihydroxyterephthalic acid in the appropriate organic solvent inside a Teflon-lined autoclave, followed by heating at the appropriate temperature (ca. $100\text{--}110^\circ\text{C}$) for 2-3 days. The use of dimethylformamide generally reduces both temperature and reaction time²⁵ but the resulting MOF then have to be washed several days with methanol because of the strong coordination of DMF molecules to the framework nickel atoms, which prevents simple removal by vacuum treatment. If the tetrahydrofuran/water mixture is used, relatively large amount of solvents are required as well as long reaction times: in a typical procedure¹², three days at 110°C were necessary to produce 6.46 g of CPO-27-Ni (4.10 g expected after complete water removal) from 100 ml of a THF/Water (1:1) mixture.

The procedure described here for the synthesis of $\text{Ni}_2(\text{dhtp})$ entails only concentrated aqueous solution under atmospheric pressure, without the addition of organic co-solvent at any point of the procedure.

H_4dhtp synthesis

2,5-dihydroxyterephthalic acid has been directly synthesized in good yields from the inexpensive hydroquinone using an organic solvent-free procedure (see **Scheme 2**), derived from a patented process²⁶ and adapted for laboratory-scale experiment by replacing pressurized CO_2 with an atmospheric-pressure

CO₂ stream. Preformed potassium formate has also been replaced by its *in situ* generation from K₂CO₃ and HCOOH to yield the molten salt reaction medium. The yellow crystalline 2,5-dihydroxyterephthalic acid can be conveniently recovered by filtration after acidification of the reaction crude and washings by water, and used directly for the MOF synthesis.



* Mixture of K₂CO₃/KHCO₃/HCOOK obtained *in situ* by adding HCOOH to an excess of solid K₂CO₃.
Scheme 2: Reaction scheme for the synthesis of 2,5-dihydroxyterephthalic acid by dicarboxylation of hydroquinone.

Ni₂(dhtp) synthesis

The procedure for Ni₂(dhtp) synthesis consists in mixing an aqueous solution of nickel (II) acetate (warmed at 80°C to allow high concentration of the metal, typically 1M) with a suspension containing 1.02 equivalent of 2,5-dihydroxyterephthalic acid in water (ca. 25 g/L). Upon adding the nickel-containing solution to the linker suspension, the reaction mixture immediately turns into a clear emerald green solution. When this solution is heated at reflux temperature, a yellow solid quickly precipitates. After 1h-reflux, washing with water and drying at 80°C, the final product is recovered as a yellow powder with almost full conversion with respect to the nickel salt, the limiting reagent of the procedure (calculated yield : 91.6%).

X-Ray Diffraction

The X-ray powder diffraction (XRD) pattern of the product after full rehydration shows a highly crystalline material (see **Figure 1** for experimental and simulated diffractograms).

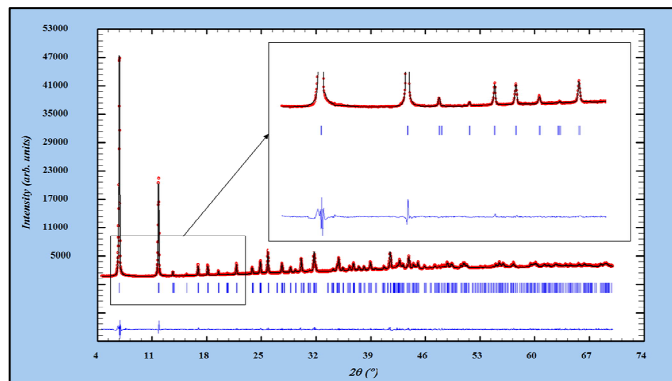


Figure 1: View of the experimental powder XRD pattern (red dots) and the simulated one (black line) by the Le Bail method. The difference curve is shown in blue.

The highest intensity peaks of the material obtained from the aqueous procedure are found at $2\Theta = 6.8^\circ$ and 11.8° (corresponding to $d_{hkl} = 12.99 \text{ \AA}$ and 7.48 \AA). These measurements are in good agreement with the published CPO-

27-Ni crystallographic data²² : $2\Theta = 6.80^\circ$ and 11.79° , corresponding to $d_{hkl} = 12.99 \text{ \AA}$ and 7.50 \AA , that is the (-120) and (030) planes, respectively. The X-ray powder diffraction pattern was fitted using Le Bail full profile fitting method²⁷ through the FullProf²⁸ and Winplotr²⁹ softwares. **Figure 1** shows a good agreement between the recorded powder pattern (red) and the simulated one (black). No supplementary peaks were observed in the difference curve (blue) which confirms the purity of the obtained sample.

Permanent microporosity

The reversible N₂ adsorption and desorption performed at 77K (see **Figure 2** and **Figure S1**) lead to specific surface areas of 1233 m²/g (Brunauer-Emmett-Teller (BET) method) and 1355 m²/g (Langmuir method), in line with the highest specific surface area of 1218 m²/g (BET method) reported in the literature for CPO-27-Ni material¹². The adsorption/desorption isotherms are satisfactorily fitted with the NLDFT simulation method³⁰ (see **Figure S1**), which allows to obtain a pore size distribution plot (see inset **Figure 2**) with a mean pore diameter of 11.7 Å, in agreement with the calculated value of 11.85 Å¹², and an estimated pore volume of 0.823 cm³/g.

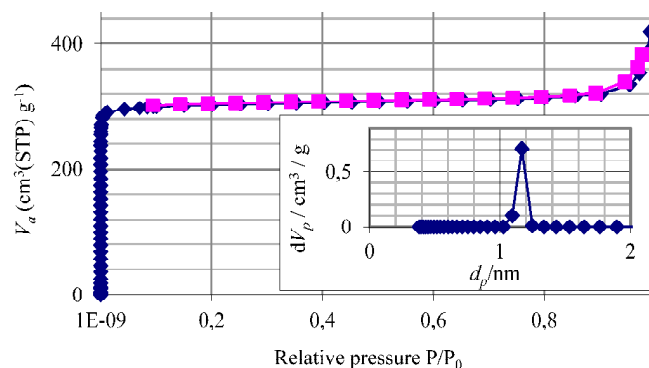


Figure 2: Experimental N₂ adsorption (blue diamonds) and desorption (purple squares) isotherms at 77K of Ni₂(dhtp) synthesized in aqueous solution; in the inset: calculated pore size distribution from simulated adsorption isotherm reported in Supplementary information, **Figure S1**.

Magnetic susceptibility

The magnetic behavior of the Co³¹ and Fe³² members of the M₂(dhtp) isomorphous family of MOFs has already been reported, but not, to the best of our knowledge for Ni₂(dhtp), for which only a theoretical investigation is available³³. At room temperature, the product of the magnetic susceptibility with the temperature (χT), of a fully rehydrated Ni₂(dhtp) obtained from the water based route, is 2.67 cm³.K.mol⁻¹. Upon cooling, χT increases and reaches the maximum value of 3.57 cm³ K mol⁻¹ at 20 K and then drops abruptly below this temperature. This behavior is in agreement with the ferromagnetic coupling of nickel (II) ions ($S = 1$) along the chain running parallel to the *c* axis, as previously observed for Co(II) and Fe(II) analogs^{31, 32}. To extract the value of the magnetic interaction, the data were simulated for [Ni₂(dhtp)(H₂O)₂]·8H₂O assuming Heisenberg

interactions between spins ($H = -2J\sum S_i S_{i+1}$) using the Fisher analytical expression for the magnetic susceptibility of an infinite chain of classical spins $S = 1$ with an interchain magnetic interaction in the molecular field approximation (ZJ')^{34, 35}. The best fit (**Figure 3A**) gives a ferromagnetic intrachain interaction $J = +8.1 \text{ cm}^{-1}$ and an antiferromagnetic interchain interaction $J' = -1.15 \text{ cm}^{-1}$ with $Z = 3$ as previously suggested³² and $g = 2.02$. A small TIP has been included ($150 \cdot 10^{-6} \text{ cm}^{-1}$). At 2K the magnetization vs. magnetic field (**Figure 3B**) first increases linearly with the magnetic field. Then, around 2.8 T, a transition is observed, progressively moving towards the expected value for two nickel (II) ions ($\approx 2\mu_B$). This field-induced transition may be ascribed to the fact that the small antiferromagnetic interchain interactions are overtaken by the strength of the magnetic field, in line with what has already been reported for the CPO-27-Co³¹.

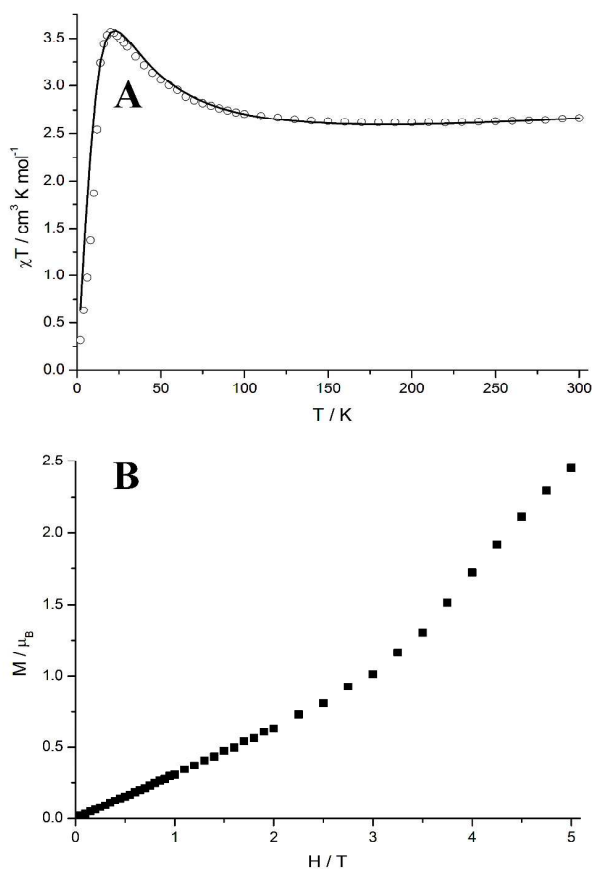


Figure 3: **A:** Temperature dependence of χT for $[\text{Ni}_2(\text{dhtp})(\text{H}_2\text{O})_2] \cdot 8\text{H}_2\text{O}$. The solid line is the best fit of experimental data with the parameters reported in the text; **B:** Magnetization curves for $[\text{Ni}_2(\text{dhtp})(\text{H}_2\text{O})_2] \cdot 8\text{H}_2\text{O}$.

Thermal behavior

Thermogravimetric analysis under N_2 of another aliquot of the $\text{Ni}_2(\text{dhtp})$ material exposed to moist air at room temperature for thirty minutes displays both of the expected phenomena²², namely: *firstly*) a loss of water molecules present inside the pores of the MOF or coordinated to the nickel atom, phenomenon occurring up to 200°C and leading to the fully

dehydrated phase, $\text{Ni}_2(\text{dhtp})$, which is stable up to 360°C , and *secondly*) the thermal decomposition of MOF material (see **Figure S2 A**). The water content estimated from the weight loss up to 200°C is equivalent to about 8 molecule of water per $\text{Ni}_2(\text{dhtp})$, suggesting an almost complete rehydration of the sample toward its fully hydrated form $[\text{Ni}_2(\text{dhtp})(\text{H}_2\text{O})_2] \cdot 8\text{H}_2\text{O}$ reported in the literature¹². As already reported, the thermogram obtained under O_2 is quite similar, with decomposition occurring at lower temperature (280° vs. 360°C under N_2 , see **Figure S2 B**).

Morphology of the $\text{Ni}_2(\text{dhtp})$ synthesized in water

The well-formed 1D channels of the $\text{Ni}_2(\text{dhtp})$ material obtained from the aqueous synthetic route were observed by high-resolution transmission electron microscopy (see **Figure 4A**). The measured 12.5 \AA distance between two contiguous lines observed in the micrograph can be explained as corresponding to the 12.99 \AA spacing between two (-120) planes in the CPO-27-Ni crystallographic structure (see **Figure S3**)²².

At lower magnification, the micrographs showed platelets of about $1 \mu\text{m}$ width (see inset in **Figure 4A**), distinctively different in morphology with respect to the crystallites obtained by us following the CPO-27-Ni procedure¹² (see **Figure 4B**).

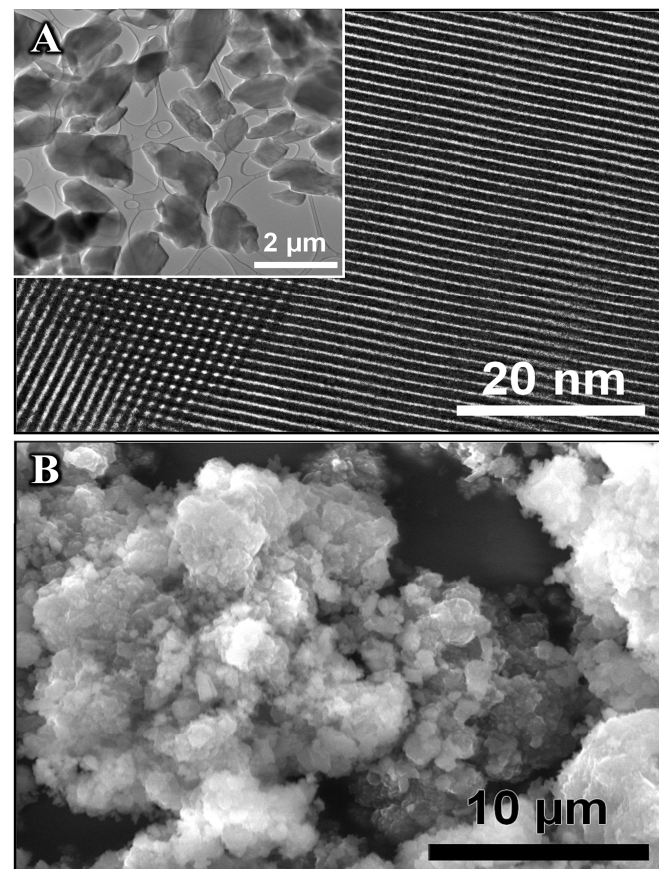


Figure 4: **A and inset:** High-resolution transmission electron micrograph at different magnification of $\text{Ni}_2(\text{dhtp})$ obtained in water; **B:** Scanning electron micrograph of $\text{Ni}_2(\text{dhtp})$ obtained in THF/water (1:1)¹².

This lower symmetry morphology with presence of agglomerates appears representative of the morphology induced by the CPO-27 route, based on the comparison with existing literature micrographs of CPO-27-Ni³⁶. As recently reviewed,³⁷ the existence of a correlation between the composition of the solvent mixture and the crystallinity, or the shape of the resulting MOF crystals has already been established for some MOFs. The use of water as a co-solvent in such strategy was directly addressed in a study on MIL-96(Al) shape-selected crystallites growth³⁸. The solvent appears in most cases to act as a modulator of crystal nucleation processes. To the best of our knowledge, such phenomenon had not yet been observed for a member of the M₂(dhtp) family.

Mechanistic considerations

Substantial interest also lies in understanding the mechanism by which the MOF self-assembles from the metal ion and the linker precursor³⁹. While we are unable to account for the crystallization mechanism that underpins the synthesis of the Ni₂(dhtp) in water, the observation of some intermediates during the synthesis appears facilitated by the mild conditions reported here. During the synthesis, we observed the complete dissolution of the otherwise sparingly soluble acid linker at room temperature (see **Figure S4 A to C**). We assign such dissolution to the deprotonation of 2,5-dihydroxyterephthalic acid (pKa estimated at ca. 2.2[†]) by the acetate counterion of the nickel salt present in the aqueous solution (pKa of acetic acid = 4.76)⁴⁰. If this emerald green mother solution is stored for few minutes at room temperature, pastel green crystals start precipitating (see **Figure S4 D**) whose X-ray diffraction pattern is different from that of CPO-27-Ni (see **Figure S5**). The final MOF can be observed only when the mixture is heated above ca. 80°C, and its formation is complete within 1h if the heating is carried out at 100°C (**Figure S4 E**).

Conclusions

In conclusion, we have reported a novel synthetic route to Ni₂(dhtp): in water, under air, at atmospheric pressure, with high space-time-yield and from an affordable linker, therefore complementing this already well-remarked member of the MOFs materials family with an additional attractive feature. A pertinent parameter to compare the performance of the aqueous route described herein with respect to the previously reported ones in organic solvents is the space-time yield expressed in terms of isolated MOF weight / volume of solvent used / time unit^{10, 41, 42}. While the total volume of all solvents used should be taken into consideration, the available published data allow to calculate this value only taking into account the volume used during the synthesis itself (and not the ones used for the washing steps). The procedure reported here yields a production rate of 28.5 g/L/h, that is a 50-fold increase with respect to the published route (0.6 g/L/h considering the weight of fully dehydrated Ni₂(dhtp))¹². Expressed in Kg/m³/day, the industrially pertinent unit, the space-time yield of the water-

based route described here could be extrapolated to 680 Kg/m³/d; such figure should be considered only as a very high upper estimate, since we have tested our method only on a 18g-scale and have not included the time-intensive washing and drying steps necessary for the ton-scale batches. At the same time, such figure abodes well of the industrial potential of this route, given the reported industrial space-time yields of 160 Kg/m³/d for Basolite A100[®], 225 Kg/m³/d for Basolite C300[®] and over 300 Kg/m³/d for Basolite M050^{®41}.

Acknowledgements

We are grateful to Ruben Vera from the “Centre de Diffractométrie Henri Longchambon” (Université Claude Bernard Lyon 1) for XRD measurements, to Erwann Jeanneau from the “Centre de Diffractométrie Henri Longchambon” for the Le Bail refinement of PXRD pattern, and to Ruben Checa from the “Laboratoire des Multimatiériaux et Interfaces” (Université Claude Bernard Lyon 1) for magnetic susceptibility measurements.

Author Contributions

The manuscript was written through contributions of all authors.

Funding Sources

“Centre National de la Recherche Scientifique” (CNRS), “Ecole Supérieure de Chimie, Physique et Electronique de Lyon” (CPE Lyon) and “Université Claude Bernard Lyon 1” (UCBL) are kindly acknowledged for support.

Experimental Section

Materials and methods

Nickel (II) acetate tetrahydrate 99%, (Sigma-Aldrich), hydroquinone (Aldrich Chemie), anhydrous K₂CO₃ (Acros), formic acid 98% (Sigma-Aldrich) and HCl 37% (VWR Chemicals) were used without further purification.

Characterization techniques

Powder X-ray diffraction data were collected in the “Centre de Diffractométrie Henri Longchambon”, site CLEA, Villeurbanne, on Bruker D8 Advance Diffractometer (Cu K α radiation, 33 kV, 45 mA). Diffraction data were recorded in the range of 4-70° 2 θ . **High-Resolution Transmission Electron Micrographs** were performed at the “Centre Technologique des Microstructures”, UCBL, Villeurbanne, on Jeol 2100F Transmission Electron Microscope. The acceleration voltage was 200 kV. **Scanning Electron Micrographs** were performed at the “Centre Technologique des Microstructures”, UCBL, Villeurbanne, on FEI Quanta 250 FEG scanning electron microscope. **Nitrogen adsorption/desorption measurements** were carried out at 77K using a BELSORB-max from BEL JAPAN system. Before N₂ adsorption, the samples were outgassed at 2.5*10⁻⁵ Pa ; 423 K for 3h. **¹H and ¹³C liquid NMR spectra** were recorded on a Bruker DSX 300 NMR

spectrometer. **Magnetic-susceptibility data** (2 - 300 K) were collected with a Quantum Design MPMS SQUID magnetometer under an applied magnetic field of 0.1 T on a powdered polycrystalline sample pressed in a PTFE sample holder equipped with a piston to avoid dehydration. The magnetization isotherm was collected at 2 K between 0 and 5 T. All data were corrected with the contribution of the sample holder and diamagnetism of the sample estimated with Pascal's constants³⁵. The analysis of magnetic data was carried out by simulation of χT thermal dependence including an intramolecular interaction (J), an intermolecular interaction (zJ') in the molecular field approximation and a temperature independent paramagnetism (TIP) according to the following expression:

$$\chi = \frac{kg_{iso}^2 F(J,T)}{12kT - 16zJ'F(J,T)} + TIP$$

$$\text{Where } F(J,T) = 2 \frac{(1-u)}{(1+u)} \quad \text{and} \quad u = \frac{kT}{4J} - \coth \frac{4J}{kT}$$

Unless otherwise specified, all analyses were performed on fully rehydrated Ni₂(dhtp) samples. The rehydration procedure consisted in exposing the material (previously dried at 80°C overnight and stored in dry box) to water-saturated air for 24h at room temperature.

Preparation of 2,5-dihydroxyterephthalic acid from hydroquinone

In a 500 ml 2-neck round-bottom flask equipped with a condenser, K₂CO₃ (97.7 g, 0.7 mol) was introduced. Formic acid (42.3 g, 0.9 mol) was added drop by drop under robust magnetic stirring, releasing large amount of CO₂ and causing a strong exothermicity. The mixture was then heated up to 210°C, leading to a thick melt of potassium formate, bicarbonate and carbonate. The condenser was then removed and the reactor flushed for 30 min with a continuous stream of argon. The argon line was then replaced by a 500ml round-bottom flask filled with 300 g of dry ice. Hydroquinone (22.24 g, 0.2 mol) was added in a single portion to the melt and the condenser was placed back on the top of the reactor. The reaction mixture was then vigorously stirred for 6h at 210°C under the CO₂ stream generated by the dry ice. After 6h, the yellow reaction mixture was dispersed in 300 ml of boiling water, leading to a suspension of white crystals in a dark-brown solution. This suspension was cooled to RT and filtered. The off-white powder obtained was finally suspended in 200 ml of water and acidified with 40ml of HCl 37%, causing the suspension to turn canary yellow. This suspension was stirred for 1h, filtered and washed 3 times with 50 ml-portions of deionized water. The yellow product obtained was dried at 80°C, yielding 20.8 g (105 mmol, 52.5% based on hydroquinone) of 2,5-dihydroxyterephthalic acid which was characterized by ¹H and ¹³C NMR spectroscopy (see **Figure S6 A and B**).

¹H NMR (300 MHz, DMSO-d₆) δ = 7.28 ppm (2H, S); ¹³C NMR (300 MHz, DMSO-d₆) δ = 170.62; 152.26; 119.37; 117.52 ppm

Synthesis of Ni₂(dhtp) in water

In a 500 ml round-bottom flask equipped with a condenser, a suspension of dihydroxyterephthalic acid (10.31 g, 51 mmol) in deionized water (400 ml) was heated to reflux under strong magnetic stirring (oil bath at 160°C). In a separate flask, nickel acetate tetrahydrate (25.14 g, 100 mmol) was dissolved in deionized water (100 ml) at 80°C. The light green nickel solution obtained was dropped in one portion to the boiling dihydroxyterephthalic acid suspension under continuous stirring leading almost instantaneously to a homogeneous emerald green solution. After few minutes, a yellow precipitate started to form. The reaction mixture was further refluxed for 1h. The final suspension was filtered and the yellow microcrystalline powder washed three times with 100 ml-portions of warm deionized water before being dried overnight at 80°C. 17.90 g of this material were isolated and characterized by powder XRD, HRTEM and TGA. The microporosity was determined by N₂ adsorption at 77K after activation of a 105.7 mg aliquot for 20h at 150°C ; 5.10⁻⁵mbar. The weight loss observed during this activation process was used to determine the water content in the isolated material (4.42 water molecule per Ni₂(dhtp) unit). Isolated yield: 91.6% based on 17.90 g of [Ni₂(dhtp)·4.42 H₂O].

Notes and references

† Calculated using Advanced Chemistry Development (ACD/Labs) Software V11.02 (© 1994-2014 ACD/Labs)

- G. Ferey, *Chemical Society Reviews*, 2008, **37**, 191-214.
- M. Gaab, N. Trukhan, S. Maurer, R. Gummaraju and U. Müller, *Microporous and Mesoporous Materials*, 2012, **157**, 131-136.
- G. Ferey, M. Lacroche, C. Serre, F. Millange, T. Loiseau and A. Percheron-Guegan, *Chemical Communications*, 2003, 2976-2977.
- L. Bromberg, Y. Diao, H. Wu, S. A. Speakman and T. A. Hatton, *Chemistry of Materials*, 2012, **24**, 1664-1675.
- Y. Pan, Y. Liu, G. Zeng, L. Zhao and Z. Lai, *Chemical Communications*, 2011, **47**, 2071-2073.
- Q. Yang, S. Vaesen, F. Ragon, A. D. Wiersum, D. Wu, A. Lago, T. Devic, C. Martineau, F. Taulelle, P. L. Llewellyn, H. Jobic, C. Zhong, C. Serre, G. De Weireld and G. Maurin, *Angewandte Chemie International Edition*, 2013, **52**, 10316-10320.
- S. J. Geier, J. A. Mason, E. D. Bloch, W. L. Queen, M. R. Hudson, C. M. Brown and J. R. Long, *Chemical Science*, 2013, **4**, 2054-2061.
- X. Wu, Z. Bao, B. Yuan, J. Wang, Y. Sun, H. Luo and S. Deng, *Microporous and Mesoporous Materials*, 2013, **180**, 114-122.
- E. J. García, J. P. S. Mowat, P. A. Wright, J. Pérez-Pellitero, C. Jallut and G. D. Pirngruber, *The Journal of Physical Chemistry C*, 2012, **116**, 26636-26648.
- G. D. Pirngruber and P. L. Llewellyn, in *Metal-Organic Frameworks - Applications from Catalysis to Gas Storage*, ed. D. Farrusseng, Wiley-VCH Verlag GmbH & Co. KGaA, 2011, pp. 99-119.
- D. Yu, A. O. Yazaydin, J. R. Lane, P. D. C. Dietzel and R. Q. Snurr, *Chemical Science*, 2013, **4**, 3544-3556.
- P. D. C. Dietzel, P. A. Georgiev, J. Eckert, R. Blom, T. Strassle and T. Unruh, *Chemical Communications*, 2010, **46**, 4962-4964.
- S. Chavan, F. Bonino, L. Valenzano, B. Civalieri, C. Lamberti, N. Acerbi, J. H. Cavka, M. Leistner and S. Bordiga, *The Journal of Physical Chemistry C*, 2013, **117**, 15615-15622.

14. D. Peralta, G. Chaplais, A. Simon-Masseron, K. Barthelet and G. D. Pirngruber, *Energy & Fuels*, 2012, **26**, 4953-4960.
15. J. Liu, J. Tian, P. K. Thallapally and B. P. McGrail, *The Journal of Physical Chemistry C*, 2012, **116**, 9575-9581.
16. A. C. Kizzie, A. G. Wong-Foy and A. J. Matzger, *Langmuir*, 2011, **27**, 6368-6373.
17. J. Liu, Y. Wang, A. I. Benin, P. Jakubczak, R. R. Willis and M. D. LeVan, *Langmuir*, 2010, **26**, 14301-14307.
18. J. A. Mason, M. Veenstra and J. R. Long, *Chemical Science*, 2014, **5**.
19. L. Mitchell, B. Gonzalez-Santiago, J. P. S. Mowat, M. E. Gunn, P. Williamson, N. Acerbi, M. L. Clarke and P. A. Wright, *Catalysis Science & Technology*, 2013, **3**, 606-617.
20. S. Rojas, P. S. Wheatley, E. Quartapelle-Procopio, B. Gil, B. Marszalek, R. E. Morris and E. Barea, *CrystEngComm*, 2013, **15**, 9364-9367.
21. P. Horcajada, R. Gref, T. Baati, P. K. Allan, G. Maurin, P. Couvreur, G. Férey, R. E. Morris and C. Serre, *Chemical Reviews*, 2011, **112**, 1232-1268.
22. P. D. C. Dietzel, B. Panella, M. Hirscher, R. Blom and H. Fjellvag, *Chemical Communications*, 2006, 959-961.
23. T. Grant Glover, G. W. Peterson, B. J. Schindler, D. Britt and O. Yaghi, *Chemical Engineering Science*, 2011, **66**, 163-170.
24. E. Haque and S. H. Jung, *Chemical Engineering Journal*, 2011, **173**, 866-872.
25. D. J. Tranchemontagne, J. R. Hunt and O. M. Yaghi, *Tetrahedron*, 2008, **64**, 8553-8557.
26. A. M. Reichwein and D. J. Sikkema, Akzo Nobel N.V., 2000.
27. A. Le Bail, H. Duroy and J. L. Fourquet, *Materials Research Bulletin*, 1988, **23**, 447-452.
28. J. Rodriguez-Carvajal, in *Collected Abstracts of Powder Diffraction Meeting*, Toulouse, France, 1990, pp. 127-128.
29. J. Rodriguez-Carvajal and T. Roisnel, *Commission on Powder Diffraction, International Union of Crystallography*, 1998, Newsletter No. **20**, 35.
30. C. M. Lastoskie, *A statistical mechanics interpretation of the adsorption isotherm for the characterization of porous sorbents*, Cornell University, May, 1994.
31. P. D. C. Dietzel, Y. Morita, R. Blom and H. Fjellvåg, *Angewandte Chemie International Edition*, 2005, **44**, 6354-6358.
32. E. D. Bloch, W. L. Queen, R. Krishna, J. M. Zadrozny, C. M. Brown and J. R. Long, *Science*, 2012, **335**, 1606-1610.
33. P. Canepa, Y. J. Chabal and T. Thonhauser, *Physical Review B*, 2013, **87**, 094407.
34. M. E. Fisher, *American Journal of Physics*, 1964, **32**, 343-346.
35. O. Kahn, *Molecular Magnetism*, Wiley-VCH, New York, NY, 1993.
36. M. Tagliabue, C. Rizzo, R. Millini, P. C. Dietzel, R. Blom and S. Zanardi, *J Porous Mater*, 2011, **18**, 289-296.
37. M. Sindoro, N. Yanai, A.-Y. Jee and S. Granick, *Accounts of Chemical Research*, 2013, **47**, 459-469.
38. M. Sindoro, A.-Y. Jee and S. Granick, *Chemical Communications*, 2013, **49**, 9576-9578.
39. G. Férey, M. Haouas, T. Loiseau and F. Taulelle, *Chemistry of Materials*, 2013, **26**, 299-309.
40. D. R. Lide, *CRC Handbook of Chemistry and Physics, 90th Edition*, CRC Press, Boca Raton (Fla.); London; New York, 2009.
41. A. U. Czaja, N. Trukhan and U. Muller, *Chemical Society Reviews*, 2009, **38**, 1284-1293.
42. A. Garcia Marquez, P. Horcajada, D. Grosso, G. Férey, C. Serre, C. Sanchez and C. Boissiere, *Chemical Communications*, 2013, **49**, 3848-3850.

Synopsis TOC

Highway to MOF Ni₂(dhtp)! 1-hour in boiling water under atmospheric pressure; a cheap synthesis of the linker is also reported.

